Profiling and Optimizing the Geometric Accuracy of Additively Manufactured Components via Self-Organizing Map

Mojtaba Khanzadeh[1], Ruholla Jafari Marandi[1], M.Samie Tootooni[2], Linkan Bian[1] †, Brian Smith[1], Prahalad Rao[2]

[1]Department of Industrial and Systems Engineering, Mississippi State University, Mississippi State, MS, 39762

[2]Department of Systems Science and Industrial Engineering, Binghamton University, New York, NY 13902

Abstract

One main challenge of additive manufacturing is the lack of geometric accuracy of the parts. Part geometry measurements generated using Next Engine 3D scanners yields an extremely large amounts of data. The generated data is so large, that it is difficult to characterize and quantify the geometric accuracy of the part directly. Self-Organizing Map is utilized to investigate the major types of geometric deviations.

I. Introduction

Additive Manufacturing (AM) enables the fabrication of complex and customized parts based on Computer Aided Design (CAD) models via layer upon layer depositing of broad range of metals, composites, and plastics ([(Y. Huang et al. 2015),(W. Gao et al. 2015),(Thompson et al. 2015),(Ameta et al. 2015)]). Although AM provides several advantages, such as reduction of material waste, fabrication of complex geometries, and heterogeneous compositions ([(Y. Huang et al. 2015), (Thompson et al. 2015),(Moylan, Cooke, and Jurrens 2012)]), over traditional 'subtractive' manufacturing methods, lack-of-geometric- accuracy and surface finish of the fabricated parts with AM are major issues, which are obstacle in widespread acceptance of additive processes [(Moylan, Cooke, and Jurrens 2012)]. Existing standard methods including: ASME, ANSI, and etc. has been applied to resolve the geometric accuracy problems, but these approaches are not able to account for entire information that are hidden in complicated and new shapes. Hence, there is a lack of understanding about the different type of geometric deviations affected by process parameters, geometric designs, etc. Therefore, there is an urgent need to develop a methodology to characterize the types of geometric deviations, and to establish the relationship between process design parameters and geometric deviations.

We categorize the existing literature of geometric accuracy measurements into three major categories: (i) Geometry Optimization based on empirical deviation examinations [(Wong and Hernandez 2012)] and ASME/ANSI standards [(Schleich et al. 2014)], (ii) Simulation based approaches such as Finite Element Method (FEM), and (iii) shape compensation.

In previous studies, [(Davidson et al. 2005)] applies ASME features like Geometric Dimensions and Tolerances (GD&T) to extract the geometric information on the designed part, and relate them to design parameters. GD&T is a system for defining and communicating engineering accuracies. Commonly used GD&T features are flatness, straightness, thickness, circularity, parallelism, perpendicularity, angularity, run out, etc. These features are suitable for meaningful and diagnosable regions. For example, the deviation in different shapes like circle and cylinder can be extracted; however, one of the important drawbacks of this method is the fact that these features cannot tackle non-geometric information, which defined as shapes with irregular contours, and whose edges are not straight, nor can it consider small portion of them [(J. Gao et al. 2005)]. In

other words, the mentioned features cannot account for complex and new shapes. Furthermore, using same ASME variables is not able to distinguish geometric quality of different parts. Also, linking the (GD&T)'s to design and process parameters is a multi-objective optimization process, which has two major limitations: first, it requires plenty of experiments due to a large number of parameters that controls the AM processes to define an objective function. Second, using limited number of experiments to approximate the optimal solution brings about significant uncertainty. The known disadvantages of these methods do not end here, among others, expensive data usage for quantifying inaccuracy features, complex and tedious calculations of accuracy analysis, which make the method time-consuming and prone to error [(Chase et al. 1996)].

Additionally, quite a few simulation based approaches such as Finite Element (FE) are studied for realization of contingent relation of physical process parameters and finished part quality specifically geometric accuracy ([(King, W. E. 2015), (Xu and Chen 2015), (Pal et al. 2013), (Tapia and Elwany 2014), (Paul, Anand, and Gerner 2014)]). FE is a three-dimensional thermo-mechanical method that accounts for the thermal deformation in AM parts based on slice thickness, part orientation, scanning speed, and material properties [(King, W. E. 2015)]. In particular, thermal deformation occurs during the solidification process of each layer. Such effects are accumulated and amplified through multiple deposited layers and eventually result in distortion and shrinkage of the final parts ([(Q. Huang et al. 2014), (Wang, W. L. 1996)]); this impacts geometric and dimensional properties. However, the captured results of simulation methods are far away from the practical results and more experiments preferred to achieve the real world outcomes. Furthermore, different types of statistical and empirical methods that have been found to assess the accuracy of AM processes ([(Campanelli et al. 2007), (Zhou et al. 1999), (Onuh and Hon 2001)]), are hardly authoritative for new and inexperienced geometries.

Recently, there are several additional studies dedicated to analyze the geometric accuracy of parts and their finished surface, is shape compensation ([(Q. Huang 2016), (Q. Huang et al. 2014), (Xu, Lijuan 2013)]) that facilitates the quality measurement, online monitoring, and feedback examination of geometric accuracy. This procedure, at first, demonstrates optimal compensation strategy for two-dimensional (2D) shape deformation, then upgrades the results to 3D [(Xu, Lijuan 2013)]. However, these methods are prone to explore the well-known model for complicated shapes, due to considering inter-layer interaction in specific cross-sections and also assuming identically independent distribution for errors of different cross-sections.

Our objective is developing a novel methodology to quantify the geometric deviations of fabricated parts, profile them in feasible number of groups, and link them to process design parameters. We apply a Self-Organizing Map to cluster the different types of geometric inaccuracies. Unlike ASME, we can measure the geometric accuracy of complex parts and with less amount of scanned data. Also, our method's uncertainty is less than the simulation based FEM approach. At first, the SOM clustering procedure applied to categorize the geometric deviation data in different points. Secondly, we use a probabilistic occurrence of each cluster concept to calculate the expected value of error in fabricated part, analyze the accuracy of various process parameters, and also achieve a criterion to compare the scale of accuracy in the part. At last, preference ranking correlation technique is further developed to discern the precision of changes in data usage compared to fully scanned data. The results are validated using a part with specific shape fabricated using Fused Depositing Model (FDM), as shown in Figure 1. The geometric accuracy data is obtained via is the NextEngine HD laser scanner. The QA Scan 4.0 software is used to obtain the GD&T quantifiers directly from the laser scanned point cloud data.

The remaining of this paper is organized as follows: in section (II), we will describe the deviation measurement procedure and different process parameter combination, and also we will present the data generation flow. In section (III), we will introduce the SOM, clustering method, and its applications, then we will apply the method to formulate our problem, train a specific network for big data problems, and eventually in the last part of this section we will discuss the obtained numerical results according to the method. At last, we will illustrate sensitivity analysis based on amount of data usage and its impact on decision making to find appropriate set of process parameters (Infill, Temperature).

II. Form Accuracy Measurement of AM Parts

The experiments and measurements generate a tremendous amount of data pertaining to the form accuracy of parts. Text-format files saving the data takes 901 MB of digit space and the data has 18,098,301 rows corresponding to 12 different process parameters. Each row of data is a representation of a geometric deviation found in the part produced by one of the process parameters. Beside the process parameter identification, they have 6 columns indicating the xyz coordination of the geometric deviation, and the extent of the geometric deviation on each of the three axes. To generate this data 12 different, but identical parts, shown in Figure 1, have been produced and scanned later to find the geometric deviations and their coordination. Overall, the data has three important features the process parameters, geometric deviation's coordination, and geometric deviation severity. The following Table I introduces the types of different process parameters and the total number of geometric deviations they have. Parameter combination at Row 3 in Table I results in the lowest number of geometric deviation. However, the magnitude of geometric deviation is not taken into account, and considering only number of geometric deviations and also ASME measurements cannot explain the accuracy of multiple couple of process parameters because of the issue of distinguishability in mentioned measurements. However, there is a need to figure out different types of geometric deviations and their severity before reaching a conclusion.

Table 1.Different Process parameters

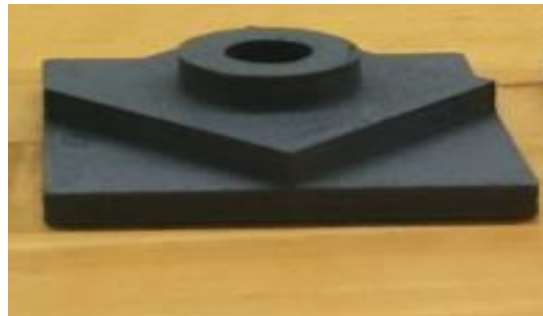| PP ID	Temperature (°F)	Infill (%)	N. geometric deviations (rows)
1	225	80	1,712,653
2	225	90	1,107,267
3	225	100	685,961
4	230	80	1,250,357
5	230	90	1,619,690
6	230	100	1,796,948
7	235	80	1,795,849
8	235	90	1,758,031
9	235	100	1,692,290
10	240	90	2,211,521
11	220	90	1,233,867
12	230	70	1,233,867

Figure 1. Fabricated part's geometry

III. Self-Organizing Map (SOM)

Self-Organizing Map is a method of Artificial Neural Networks (ANN) for unsupervised tasks such as clustering, for reference see [(Jafari-Marandi, Hu, and Omitaomu 2016), (Keramati, Abbas 2014)]. Its well-known graphical tools is what gives SOM a superiority over other clustering

techniques. In fact, recently and unprecedentedly the transparency of SOM has made the unsupervised ANN applicable for more supervised tasks such as classification and decision makings, for reference see [(Olawoyin 2012),(Konat et al. 2015)]. In this paper, SOM's graphical tools and capacity to handle a gigantic amount of data allow us to create a decision-making procedure to characterize geometric deviation in Fused Deposition Modeling.

The SOM (Self Organizing Map) Neural Network is also known as Kohonen Neural Network system. As outlined earlier the method works best for unsupervised learning tasks and its superiority is its visual presentation of the data. SOM maps the data into a 2 dimensional space membership map [(Pratiwi 2012)]. The map with specified membership of the data is what the method outputs. Figure 2 represents a SOM network for a dataset with 3 attributes. This structure of the network could address a clustering challenge on a dataset with three attributes and 12 possible clusters. On each structure of SOM network, as shown in the Figure 2, there are three types of entities: input neurons, connecting vectors and output neurons. The vectors connect the input neurons to the output neurons, and also connect neighboring output neurons. Each vector has a weight associated with it, produced randomly in initialization and updated in training process. Based on the nature of connections in the output layer, two types of SOM map exists: quadrilateral or hexagonal. The network in figure bellow will output a quadrilateral map with at most 4 connections for each neuron with its neighbors.

Similar to any other artificial neural network, the network has a training process and before that, an initiation procedure. The initialization process basically assigns random weights between -1 to 1 to each and every connection in the network. In training process of SOM, each output dataset will be, at least once, presented to the network. The input neurons will assume the values of the presented row of data, and based on the existing weights of the connections one of the output neurons will have greater value than others. The weights of the SOM will be updated so that the best output neuron value will be selected.

In this paper a 5×5 hexagonal SOM topology has been employed. The reason for choosing this specific topology is that this topology responded well in our small experiments before the final training. A good topology for SOM has two aspects. First, the topology is wide enough to be able to distinguish and extract hidden patterns in the data. On the other hand, there is a need for the topology to be computationally and analytically computable. In other words, too big of a topology will increase the computational expense of the calculations and also will make it more difficult to analyze. With the special need for computational consideration of this paper, owing to the huge size of the data SOM needs to be exposed to, we have found that a 5×5 hexagonal SOM topology struck the perfect balance for the two aspects.
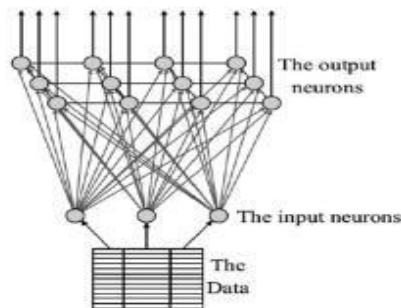

Figure 2 .Self-Organizing Map Neural Network sample [(Keramati, Abbas 2014)]

III.I. Network training process

To cluster and then profile different types of geometric deviations in the dataset, the process needs to have a holistic approach. In other words, all the 12 different process parameters, as shown in Table I, should have the same chance in shaping the network. This introduce a challenge in the training of network for this paper's dataset. The amount of data in the network is so many that it's problematic to give all the 12 process parameters the same fair chance. To introduce the existing approaches, the most simplistic way would be to start exposing the network to each and every type of data from the start to the end. This approach has the drawback of giving the first data-rows an advantage, because SOM is vulnerable to its first exposures, due to its random weighting. Another approach would be to pick randomly among all the data for each and every data-row being presented to the network. In turn, this approach suffers from the disadvantage of never being certain if all of the data-rows have been equally introduced to the system. To guard against both downsides and assuage them, a compromise in-between approaches has been selected for training the networks.

For starters, the network is exposed to a random 200 batches of 5000 data-rows from randomly selected process parameters. For every batch, each data-row in the batch is presented to the network 200 times. The reason behind this special process of randomization is the size of the data in need of processing. The data associated with each set of process parameters had to be kept in different files, and loading all the files at once would impair the computers functionality. Then, the data-rows of each set of process parameters are presented to the network 200 times. The order in which the process parameters were chosen is random. Lastly, the first random procedure of data-row selection is repeated. In total, the network is exposed to 4,019,660,200: $2 \times 200 \times 5,000 \times 200 + 18,098,301 \times 200$. It took slightly more day 4 days to train the network on a computer with 3.6 GHz CPU, and16 GB RAM.

III.II. Final decision making based on SOM

In this study, we try to profile the geometric deviations in fabricated parts with different process parameters based on their location via SOM (x, y, z) clustering method. SOM has been applied to geometric deviation data of fabricated (G_x, G_y, G_z) parts with distinctive process parameters. Figure 3 presents the membership map of SOM for only four process parameters. Every cell in Figure 3, is the possible type of geometric deviation, and the numbers in each cell accounts for number of deviation in each type. The figure illustrates that, for instance, the fabricated part with process parameter 3 has almost all different types of deviations; however, the process parameter 8 has less deviation types compared to others. These findings facilitate characterization and profiling different types of geometric deviations and also distinguishes process parameters with less deviations from others. Therefore, this kind of visualization is helpful in distinguishing geometric quality of parts based on number of deviation types on them. In our case study, fabricated parts with process parameters 8, 9, and 4 have acceptable geometric quality compare to others. However, fabricated parts with process parameters 3, 6, 10, 11, and 12 have almost all possible types of deviations and are unacceptable parts regarding to geometric quality.

The significance of this visualization outcome is the presented discrepancy with regard to the type of deviation in clusters, and also geometric accuracy of different process parameters. To measure the magnitude of deviation in each cluster, compare it with others, and concentrate the three x, y and z and values into a single value, Equation 1 proposes a magnitude measure of deviation in each point.

$$g_{ijk} = \sqrt{G_{x_{ij}}{}^2 + G_{y_{ij}}{}^2 + G_{z_{ij}}{}^2} \qquad , \begin{cases} i = 1,2,\dots,25 \\ j = 1,2,\dots,n_i \\ k = 1,2,\dots,12 \end{cases} \tag{1}$$

The Equation 1 affords us an estimation of the distribution of deviations and the average magnitude for each cluster. Applying Kolmogorov\Smirnov on deviation data of each cluster for any process parameter results in normality of distribution in every cluster, as presented in Figure 4. Additionally, it demonstrates the distribution of deviation in each cluster for different process parameters, as indicated deviations in every cluster are normally distributed. These distribution curves facilitate a few portions of deviation data to determine the geometric accuracy of a part. For instance, except magnetic, blue, pink, and green curves, which are belonging to 21, 16, 22, and 11 respectively, other curves can be accumulated in one or two clusters, and they have same effect on accuracy of various process parameters. So, these distribution curves are contributory for data reduction, and Figure 4 accounts for a data reduction section with different degree of accuracy.
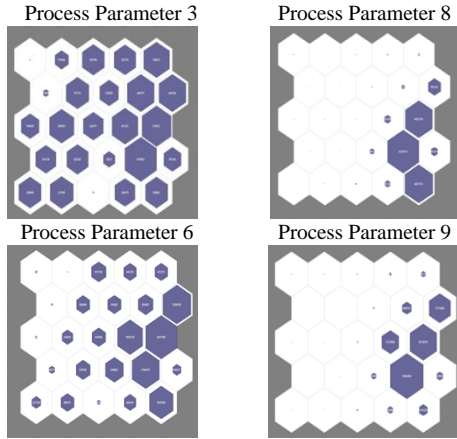
Process Parameter 3   Process Parameter 8

Process Parameter 6   Process Parameter 9

Figure 3. Demonstration of each part with different process parameters via SOM-based deviation clustering method

Process Parameter 3   *Process Parameter 8*

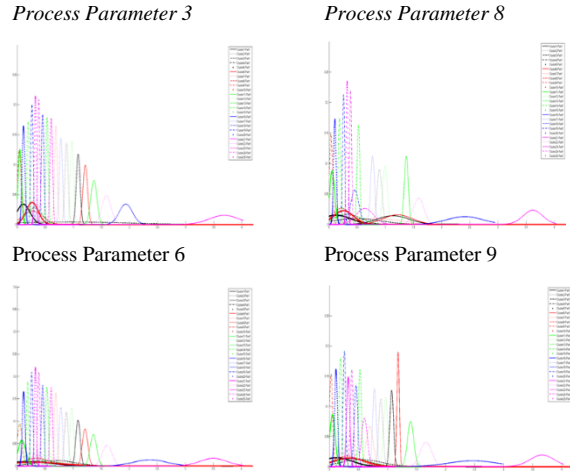Process Parameter 6   Process Parameter 9

Figure 4. Normality of geometric deviations distribution for cluster

Notation and model formulation is indicated as following:

$$G_{ik} \sim N[\mu_{ik}, \sigma_{ik}^2] \tag{2}$$

G_{ik}: Distribution of Cluster i in part k
μ_{ik}: Mean of Cluster i in part k
σ_{ik}^2: Variance of Cluster i in part k
n_{ik}: Number of data in cluster i in part k
g_{ijk}: : Deviation of point j in cluster i of part k
N_k : Number of scanned point for part k
$$N_k = \sum_{i=1}^{25} n_{ik} \tag{3}$$
P_{ik} : Incidence probability of deviation for cluster i in part k
$$P_{ik} = \frac{n_{ik}}{N_k} \tag{4}$$
E_k : Total expected value of deviation in process parameter k (Infill, Temperature)
$$E_k = \sum_{i=1}^{25} P_{ik} * \mu_{ik} \tag{5}$$
$$\mu_{ik} = \sum_{j=1}^{n_{ik}} \frac{g_{ijk}}{n_{ik}}, \; \sigma_{ik}^2 = \sum_{j=1}^{n_{ik}} \frac{(g_{ijk}-\mu_{ik})^2}{n_{ik}-1} \tag{6}$$

If we tend to compare median of different clusters statistically, it is mandatory to ensure that there is not significant disparity in variation of different clusters, hence we apply a distribution-free two-sided all treatments multiple comparisons based on pairwise rankings-general configuration test[1] [(Hollander, Myles, Douglas A. Wolfe 2013)] to test the null hypothesis of H_0: $[\tau_i = \tau_j \ \forall \ i < j]$ versus alternative hypothesis of H_a: $[\tau_i \neq \tau_j \ \forall \ i < j]$, τ_i accounts for variation in cluster i, $i = 1, 2, \ldots, 25$ within different process parameters, in significance level of $1 - \alpha = 0.95$, the conclusion is fail to reject H_0 in all 300 comparisons. Therefore, pairwise comparisons of mean values for each parts clusters are permitted because their variances' are statistically the same.

The driven results from the Equation (1-6) has been summarized in Table 2 and 3, and also and each parts' deviation magnitude and expected value of deviation for any cluster has been visualized based on resulted Tables (2,3) in Figure 5 and 6 respectively.

Table 2. Mean value of various clusters in part k for visualization in figure 4

μ_{21k}	μ_{22k}	μ_{23k}	μ_{24k}	μ_{25k}
μ_{20k}	μ_{19k}	μ_{18k}	μ_{17k}	μ_{16k}
μ_{11k}	μ_{12k}	μ_{13k}	μ_{14k}	μ_{15k}
μ_{10k}	μ_{9k}	μ_{8k}	μ_{7k}	μ_{6k}
μ_{1k}	μ_{2k}	μ_{3k}	μ_{4k}	μ_{5k}

Table 3. Expected value of Deviation in clusters of part k for visualization in figure 5

$P_{25k} * \mu_{25k}$	$P_{24k} * \mu_{24k}$	$P_{23k} * \mu_{23k}$	$P_{22k} * \mu_{22k}$	$P_{21k} * \mu_{21k}$
$P_{16k} * \mu_{16k}$	$P_{17k} * \mu_{17k}$	$P_{18k} * \mu_{18k}$	$P_{19k} * \mu_{19k}$	$P_{20k} * \mu_{20k}$
$P_{15k} * \mu_{15k}$	$P_{14k} * \mu_{14k}$	$P_{13k} * \mu_{13k}$	$P_{12k} * \mu_{12k}$	$P_{11k} * \mu_{11k}$
$P_{6k} * \mu_{6k}$	$P_{7k} * \mu_{7k}$	$P_{8k} * \mu_{8k}$	$P_{9k} * \mu_{9k}$	$P_{10k} * \mu_{10k}$
$P_{5k} * \mu_{5k}$	$P_{4k} * \mu_{4k}$	$P_{3k} * \mu_{3k}$	$P_{2k} * \mu_{2k}$	$P_{1k} * \mu_{1k}$

Figure 5 uses the membership map of SOM to illustrate the different type of deviations in various parts with calculating the magnitude of each type, as shown in Table 2, and Equation 6. The dark colors display major deviations. By comparing the colors in various clusters and different parts, it is apprehensible that clusters 21, 16, 22, and 11 are the major deviations respectively for every part, hence this visualization helped us to characterize the severity and type of deviation within clusters. However, comparing geometric accuracy of various process parameters is not applicable due to disregarding of number of deviation for different clusters. Therefore, the number of geometric deviation in each cluster is an important indicator for geometric quality of part, and we apply this criterion in coming section in Figure 6.
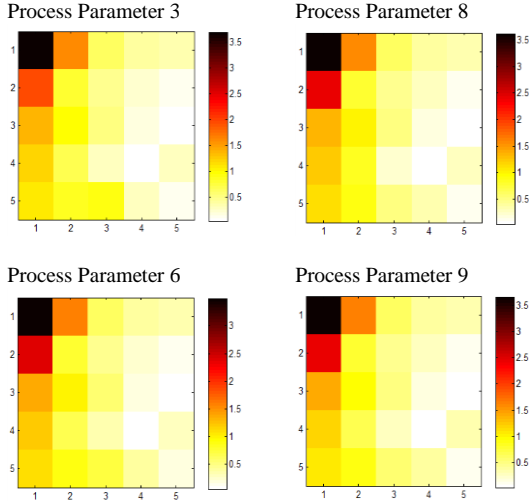
---

[1] DWASS,STEEL, AND CRITCHLOW-FLINGER

Figure 5. Magnitude of each deviation with corresponding Cluster

Expected Value = 0.482367
Expected Value = 0.08119973
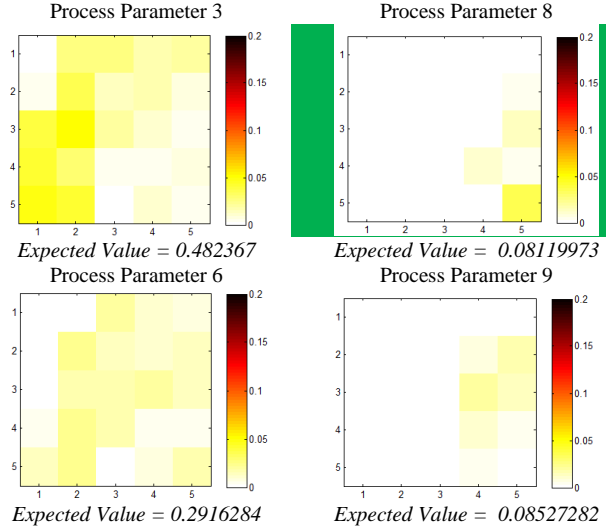Expected Value = 0.2916284
Expected Value = 0.08527282

Figure 6. Weighted magnitude of geometric deviations in each cluster for different process parameters using 100% scanned data

In Figure 6, as indicated in Table 3, we take the number of deviation in each cluster to account for calculating the incidence probability of corresponding cluster, Equation(4), then we calculate the weighted average of deviation in each cluster. In terms of visualization and color, we apply the same concept in Figure 5, but the results are totally different from Figure 5. In this visualization the geometric accuracy of various process parameters are distinguishable, for example, in Figure 5, process parameter 3 and 8 do not have obvious difference in terms of geometric accuracy by considering only type of deviations ; however, in Figure 6, process parameter 8 explicitly has more geometric accuracy compared to process parameter 3. Furthermore, the effect of major clusters are vanished in this visualization due to less number of data points. Another criterion that can be extracted based on this Figure is expected value of geometric deviation for every process parameter, as formulated in Equation 5. By comparing the calculated criterion for various process parameters optimal process parameters according to geometric accuracy are extracted as well. Therefore, coupling the mentioned approach in this section and membership map of SOM enable us to quantify the geometric accuracy of parts and distinguish geometric quality of complicated shapes with various process parameters.

IV. Sensitivity analysis

As aforementioned, the main challenge of working with this data is its colossal size. In this part we are interested to know how much of this data is actually integral in making the final decisions. The final decision that the decision making process presents is a preference ranking. Preference ranking is set of numbers from 1 to 12, which indicates the quality of part in terms of geometric accuracy for each set of process parameters. In other words, the rank will show the order of best choices among the set of process parameters using the decision making procedure. Using the whole data, the order of these choices for set of process parameters is decided to be 8, 9, 7, 4, 5, 1, 2, 12, 10, 6, 11, and 3, the couple of process parameters (Infill, Temperature) can be find in Table I in the beginning. The ranking is calculated using E_k (Total expected value of deviation in process parameter k (Infill, Temperature)) and the results are presented in Figure 6. We observed that 99.9 percent of the calculated E_k for every single row of data has value between zero and 3.5. To analyze the role of size of the data in the final decision (final rank), the following data sensitivity process was applied. First, a ranking is extracted only based on the data that has E_k greater than 3.5, which

accounts for less than 0.01 percent of the data. With the step of 0.1 in E_k value, being taken away from 3.5 in each step, 349 more rankings are made. The correlation between the ranking of the final decision and each ranking extracted in the explained procedure is presented in Figure 7. The correlation between preference ranking for various amount of data and whole data indicates how the preference rankings are similar. This diagram shows a couple of major jumps that are important in accuracy of decision making based on smaller number of our data. Using only the deviations that has E_k value greater than 1.62, which accounts for 0.1% of the data, leads to a ranking which has 0.86 correlation with the final decision. The ranking for this point is 4, 9, 8, 1, 7, 2, 5, 10, 6, 11, 12, and 3 (each number accounts for set of process parameters in Table I). Although the final decision on the best process parameters is different (4 instead of 8), this is still significant given the percentage amount of the data being used for the decision.
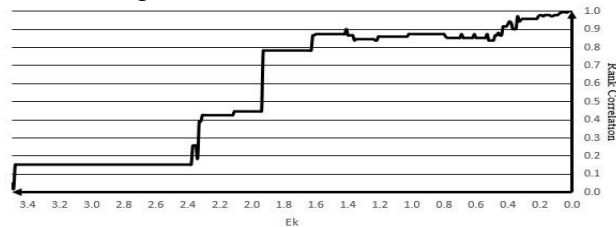

Figure 7. Data size sensitivity analysis based on E_k

To have a better understanding of the role of the percentage amount of data, Figure 8 and Figure 9 are presented. In fact, the two figures are complementary. Figure 8 magnifies the changes of correlation values when the percentages is between 0 and 4, while Figure 9 illustrates the rest. We can see that 1.6 that we earlier saw is in fact the start of the correlation value to stay above 0.85 until percentage value hits 12.1. At this level of data engagement correlation is above 0.9 and stays that way for the rest of percentages. The decision ranking is 4, 9, 8, 5, 7, 1, 2, 12, 11, 10, 6, and 3 for 12 different set of process parameters. The ranking has gotten closer to the final decision, but we are still not finding the best process parameters. At 20.8% (data usage percentage) in Figure 9, the diagram passes 0.95 correlation and stays above that for the rest of the values. The E_k value that engages this percentage of that data is 0.32 and the ranking is 8, 4, 9, 7, 5, 1, 2, 12, 11, 6, 10, and 3. This is very significant that only 21% of the data should have been kept and analyze, since the final decision of the procedure stays the same and the ranking correlation stays above 0.95.
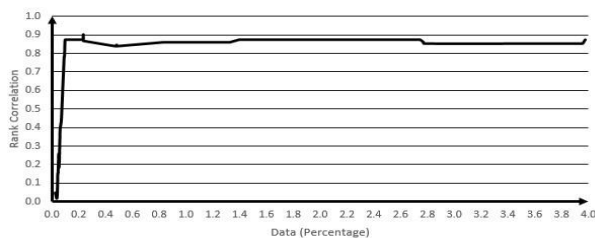

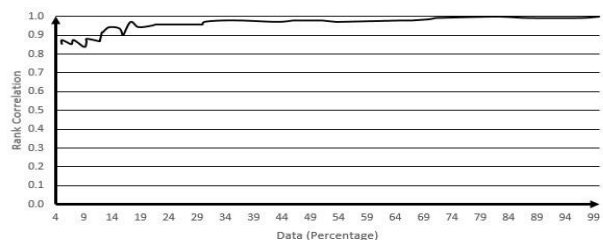Figure 8.Data size sensitivity analysis based on the data usage percentage 0-4%

Figure 9. Data size sensitivity analysis based on the data usage percentage 4-100%

V. CONCLUSION

We applied SOM clustering method to characterize/profile the geometric deviation of part with specific shape fabricated using FDM. The developed method is able to characterize the types of deviations and distinguish good-quality parts from others. It facilitates achieving optimal process parameters based upon expected value of deviation, and the obtained process parameters are unique according to magnitude of geometric deviations in part. Furthermore, our approach is capable of analyzing geometric accuracy of parts with complicated and untried geometries. Instead of

considering limited amounts of geometric dimensions and deviation criteria such as flatness, thickness, circularity, straightness, and etc., it handles the high-volume scanned data to find the severe geometric deviations, which lowers the geometric accuracy of the fabricated part. Data reduction is the most significant outcome of this research because it utilizes very small portion of data to approach the optimal process parameters captured with entire data rows.

References

1. Ameta, G., Witherell, P., Moylan, S., & Lipman, R. n.d. "Tolerance Specification and Related Issues for Additively Manufactured Products." *In ASME 2015 International Design Engineering Technical Conferences and Computers and Information in Engineering Conference* pp. V01AT0.

2. Campanelli, S. L., G. Cardano, R. Giannoccaro, A. D. Ludovico, and E. L J Bohez. 2007. "Statistical Analysis of the Stereolithographic Process to Improve the Accuracy." *CAD Computer Aided Design* 39 (1): 80–86. doi:10.1016/j.cad.2006.10.003.

3. Chase, Kenneth W., Jinsong Gao, Spencer P. Magleby, and Carl D. Sorensen. 1996. "Including Geometric Feature Variations in Tolerance Analysis of Mechanical Assemblies." *1IIE Transactions* 28 (10): 795–807.

4. Davidson, Joseph K., Jami J. Shah, and Amir Mujezinovié. n.d. "Method and Apparatus for Geometric Variations to Integrate Parametric Computer Aided Design with Tolerance Analyses and optimizationNo Title." *U.S. Patent No. 6,963,824.*

5. Gao, Jian, De Tao Zheng, Nabil Gindy, and Doug Clark. 2005. "Extraction/conversion of Geometric Dimensions and Tolerances for Machining Features." *International Journal of Advanced Manufacturing Technology* 26 (4): 405–14. doi:10.1007/s00170-004-2195-3.

6. Gao, Wei, Yunbo Zhang, Devarajan Ramanujan, Karthik Ramani, Yong Chen, Christopher B. Williams, Charlie C.L. Wang, Yung C. Shin, Song Zhang, and Pablo D. Zavattieri. 2015. "The Status, Challenges, and Future of Additive Manufacturing in Engineering." *Computer-Aided Design* 69. Elsevier Ltd: 65–89. doi:10.1016/j.cad.2015.04.001.

7. Hollander, Myles, Douglas A. Wolfe, and Eric Chicken. 2013. *No TitleNonparametric Statistical Methods*. John Wiley & Sons.

8. Huang, Qiang. 2016. "An Analytical Foundation for Optimal Compensation of Three-Dimensional Shape Deformation in Additive Manufacturing." *Journal of Manufacturing Science and Engineering* 138 (6): 61010. doi:10.1115/1.4032220.

9. Huang, Qiang, Jizhe Zhang, Arman Sabbaghi, and Tirthankar Dasgupta. 2014. "Optimal Offline Compensation of Shape Shrinkage for Three-Dimensional Printing Processes." *IIE Transactions* 47 (5): 431–41. doi:10.1080/0740817X.2014.955599.

10. Huang, Yong, Ming C. Leu, Jyoti Mazumder, and Alkan Donmez. 2015. "Additive Manufacturing: Current State, Future Potential, Gaps and Needs, and Recommendations." *Journal of Manufacturing Science and Engineering* 137 (1): 14001. doi:10.1115/1.4028725.

11. Jafari-Marandi, Ruholla, Mengqi Hu, and OluFemi A. Omitaomu. 2016. "A Distributed Decision Framework for Building Clusters with Different Heterogeneity Settings." *Applied Energy* 165. Elsevier Ltd: 393–404. doi:10.1016/j.apenergy.2015.12.088.

12. Keramati, Abbas, and Ruholla Jafari-Marandi. 2014. "Webpage Clustering: Taking the Zero Step—a Case Study of an Iranian Website." *Journal of Web Engineering* 13.3-4: 333–60.

13. King, W. E., et al. 2015. "Laser Powder Bed Fusion Additive Manufacturing of Metals; Physics, Computational, and Materials Challenges." *Applied Physics Reviews* 2.4 (2015).

14. Konat, Ahmed Amara, Heping Pan, Sinan Fang, Shazia Asim, Yao Yevenyo Ziggah, Chengxiang Deng, and Nasir Khan. 2015. "Capability of Self-Organizing Map Neural Network in Geophysical Log Data Classification: Case Study from the CCSD-MH." *Journal of Applied Geophysics* 118. Elsevier B.V.: 37–46. doi:10.1016/j.jappgeo.2015.04.004.

15. Moylan, S, a Cooke, and K Jurrens. 2012. "A Review of Test Artifacts for Additive Manufacturing." doi:http://dx.doi.org/10.6028/NIST.IR.7858.

16. Olawoyin, Richard O. 2012. "Application of Expert Systems in the Characterization and Impact of Petroleum Derivatives on Human Health." *ProQuest Dissertations and Theses*, no. December. http://search.proquest.com/docview/1355741493?accountid=11648.

17. Onuh, S. O., and K. K B Hon. 2001. "Improving Stereolithography Part Accuracy for Industrial Applications." *International Journal of Advanced Manufacturing Technology* 17 (1): 61–68. doi:10.1007/s001700170210.

18. Pal, Deepankar, Nachiket Patil, Mohammad Nikoukar, Kai Zeng, Khalid Haludeen Kutty, and Brent E Stucker. 2013. "An Integrated Approach to Cyber-Enabled Additive Manufacturing Using Physics Based, Coupled Multi-Scale Process Modeling." *Proceedings of the Solid Freeform Fabrication Symposium* 136 (December 2014): 1–18. doi:10.1115/1.4028580.

19. Paul, Ratnadeep, Sam Anand, and Frank Gerner. 2014. "Effect of Thermal Deformation on Part Errors in Metal Powder Based Additive Manufacturing Processes." *Journal of Manufacturing Science and Engineering* 136

(3): 31009. doi:10.1115/1.4026524.

20. Pratiwi, Dian. 2012. "The Use of Self Organizing Map Method and Feature Selection in Image Database Classification System." *CoRR*, 5. http://arxiv.org/abs/1206.0104.

21. Schleich, Benjamin, Nabil Anwer, Luc Mathieu, and Sandro Wartzack. 2014. "Skin Model Shapes: A New Paradigm Shift for Geometric Variations Modelling in Mechanical Engineering." *CAD Computer Aided Design* 50 (May 2014): 1–15. doi:10.1016/j.cad.2014.01.001.

22. Tapia, Gustavo, and Alaa Elwany. 2014. "A Review on Process Monitoring and Control in Metal-Based Additive Manufacturing." *Journal of Manufacturing Science and Engineering* 136 (6): 60801. doi:10.1115/1.4028540.

23. Thompson, Scott M., Linkan Bian, Nima Shamsaei, and Aref Yadollahi. 2015. "An Overview of Direct Laser Deposition for Additive Manufacturing; Part I: Transport Phenomena, Modeling and Diagnostics." *Additive Manufacturing* 8. Elsevier B.V.: 36–62. doi:10.1016/j.addma.2015.07.001.

24. Wang, W. L., et al. 1996. "Influence of Process Parameters on Stereolithography Part Shrinkage." *Materials & Design* 17.4 (1996: 205–13.

25. Wong, Kaufui V., and Aldo Hernandez. 2012. "A Review of Additive Manufacturing." *ISRN Mechanical Engineering* 2012: 1–10. doi:10.5402/2012/208760.

26. Xu, Lijuan, et al. 2013. "Shape Deviation Modeling for Dimensional Quality Control in Additive Manufacturing." *ASME 2013 International Mechanical Engineering Congress and Exposition*.

27. Xu, Kai, and Yong Chen. 2015. "Mask Image Planning for Deformation Control in Projection-Based Stereolithography Process." *Journal of Manufacturing Science and Engineering* 137 (3): 31014. doi:10.1115/1.4029802.

28. Zhou, Jack, Dan Herscovici, Calvin Chen, Jack G Zhou, Daniel Herscovici, and Calvin C Chen. 1999. "Parametric Process Optimization to Improve the Accuracy of Rapid Prototyped Stereolithography Parts." *International Journal of Machine Tools and Manufacture*, no. 4040: 1–17.